

# Schrödinger functional boundary conditions and improvement of the $SU(N)$ pure gauge action for $N > 3$

---

**Tuomas Karavirta\***

*CP<sup>3</sup>-Origins, IFK & IMADA, University of Southern Denmark,  
Campusvej 55, DK-5230 Odense M, Denmark.  
E-mail: karavirta@cp3-origins.net*

**Ari Hietanen**

*CP<sup>3</sup>-Origins, IFK & IMADA, University of Southern Denmark,  
Campusvej 55, DK-5230 Odense M, Denmark.  
E-mail: hietanen@cp3-origins.net*

**Pol Vilaseca**

*School of Mathematics, Trinity College Dublin,  
Dublin 2, Ireland  
E-mail: dionaea.0@gmail.com*

The leading method to study the running coupling constant of non-abelian gauge theories is based on the Schrödinger functional scheme. However, the boundary conditions and  $\mathcal{O}(a)$  improvement have not been systematically generalized for theories with more than three colors. These theories have applications in BSM model building as well as in the large  $N$  limit. We have studied the boundary conditions and improvement for the pure Yang-Mills theory within the Schrödinger functional scheme. We have determined for all values of  $N$  the boundary fields which provide high signal/noise ratio. Additionally, we have calculated the improvement coefficient  $c_t$  for the pure gauge to one loop order for  $SU(N)$  gauge theories with  $N = 2, \dots, 8$  from which  $N \geq 4$  are previously unknown.

*Preprint: CP<sup>3</sup>-Origins-2013-042 DNR90 & DIAS-2013-42*

*31st International Symposium on Lattice Field Theory - LATTICE 2013  
July 29 - August 3, 2013  
Mainz, Germany*

---

\*Speaker.

## 1. Introduction

Recently there has been an interest in the scaling properties of the gauge coupling in  $SU(N)$  theories with more than three colors [1, 2, 3]. For a review of large  $N$  gauge theories see [4]. The studies are motivated by their applications in Beyond Standard Model (BSM) physics and by the need to understand the scaling of the coupling constant in the large  $N$  limit.

The main tool for measuring the evolution of the coupling constant as a function of the scale on the lattice is the Schrödinger functional method. As is well-known this method suffers from  $\mathcal{O}(a)$  lattice artifacts that originate from the boundary terms. They can be removed by adding improvement terms to the action and tuning appropriately the improvement coefficients [5]. Until now the boundary coefficient necessary to improve the pure gauge theory was only known for  $N = 2$  and 3 [5, 6].

In these proceedings, we present the preliminary results of calculating the improvement coefficient  $c_t$  to one loop order in perturbation theory for the pure gauge theory with  $N = 2, \dots, 8$ . After implementing  $\mathcal{O}(a)$  improvement we see that the discretization effects are reduced for all considered values of  $N$ . In addition, we have done a study with a general  $N$  to find Schrödinger functional boundary fields with high signal/noise ratio that could be used in lattice simulations.

## 2. Theory

We use the standard  $\mathcal{O}(a)$  improved  $SU(N)$  Wilson gauge action in the Schrödinger functional scheme

$$S = S_G + \delta S_{G,b}, \quad (2.1)$$

where

$$S_G = \frac{1}{g_0^2} \sum_p \text{Tr}[1 - U(p)], \quad (2.2)$$

$$\delta S_{G,b} = \frac{1}{g_0^2} (c_t - 1) \sum_{p_t} \text{Tr}[1 - U(p_t)]. \quad (2.3)$$

$U(p_t)$  refer to the timelike plaquettes on the  $T = 0$  and  $T = L$  boundaries. Additionally the perturbative expansion of the improvement coefficient  $c_t$  is

$$c_t = 1 + c_t^{(1,0)} g_0^2 + \mathcal{O}(g_0^4). \quad (2.4)$$

The gauge fixing procedure leads to the addition of gauge fixing  $S_{gf}$  and Faddeev-Popov ghost  $S_{FP}$  terms to the action.

In the Schrödinger functional (SF) scheme the boundary conditions in the temporal boundaries are taken to be abelian and spatially constant [5], given by

$$U_k(t = 0, \vec{x}) = \exp[aC_k], \quad U_k(t = L, \vec{x}) = \exp[aC'_k],$$

with

$$C_k = \frac{i}{L} \text{diag}(\phi_1(\eta), \dots, \phi_n(\eta)), \quad C'_k = \frac{i}{L} \text{diag}(\phi'_1(\eta), \dots, \phi'_n(\eta)).$$

The phases  $\phi_i$  and  $\phi'_i$  depend on an internal parameter  $\eta$ . This choice of boundary conditions induces a background field which is a unique minimum of the action provided that the phases  $\phi$  and  $\phi'$  lay within the fundamental domain [5]. See Section 3 for more details. Boundary conditions in the spatial directions are taken to be periodic.

The effective action has a perturbative expansion of the form<sup>1</sup>

$$\Gamma = -\ln \left\{ \int D[\psi]D[\bar{\psi}]D[U]D[c]D[\bar{c}]e^{-S} \right\} = g_0^{-2}\Gamma_0 + \Gamma_1 + \mathcal{O}(g_0^2). \quad (2.5)$$

A renormalized coupling can be defined in the Schrödinger functional scheme as a derivative of the effective action (2.5) respect to the parameter  $\eta$ ,

$$g^2 = \frac{\partial\Gamma_0}{\partial\eta} / \frac{\partial\Gamma}{\partial\eta} = g_0^2 - g_0^4 \frac{\partial\Gamma_1}{\partial\eta} / \frac{\partial\Gamma_0}{\partial\eta} + \mathcal{O}(g_0^6). \quad (2.6)$$

In lattice studies it is common to use the lattice step scaling function  $\Sigma(u, s, L/a)$ , which describes the evolution of the renormalized coupling constant under a change of scale by a factor  $s$ :

$$\begin{aligned} \Sigma(u, s, L/a) &= g^2(g_0, sL/a)|_{g^2(g_0, L/a)=u} \\ &= u + \Sigma_{1,0}(s, L/a)u^2 + \mathcal{O}(u^3). \end{aligned} \quad (2.7)$$

We also use the function

$$\delta_0(L/a) = \frac{\Sigma_{1,0}(2, L/a)}{\sigma_{1,0}(2)}, \quad (2.8)$$

to measure the convergence of the lattice step scaling function  $\Sigma_{1,0}(2, L/a)$  to its continuum limit  $\sigma_{1,0}(2) = 2b_{0,0} \ln 2$ . In the previous equation  $b_{0,0} = 11N_c / (48\pi^2)$  is the one loop coefficient of the pure gauge  $\beta$ -function.

### 3. Boundary fields

Boundary fields  $\phi$  and  $\phi'$  are within the fundamental domain if they satisfy the equations [5]

$$\phi_1 < \phi_2 < \dots < \phi_n, \quad |\phi_i - \phi_j| < 2\pi, \quad \sum_{i=1}^N \phi_i = 0. \quad (3.1)$$

Such vectors  $\phi$  form a  $N - 1$  simplex with vertices

$$\begin{aligned} \mathbf{X}_1 &= \frac{2\pi}{N} (-N + 1, 1, 1, \dots, 1) \\ \mathbf{X}_2 &= \frac{2\pi}{N} (-N + 2, -N + 2, 2, \dots, 2) \\ \mathbf{X}_3 &= \frac{2\pi}{N} (-N + 3, -N + 3, -N + 3, 3, \dots, 3,) \\ &\vdots \\ \mathbf{X}_{N-1} &= \frac{2\pi}{N} (-1, -1, \dots, -1, N - 1) \\ \mathbf{X}_N &= (0, 0, \dots, 0). \end{aligned} \quad (3.2)$$

For SU(4) the fundamental domain is shown in figure 1.

<sup>1</sup>We refer to the original literature [5] for details on the perturbative expansion of the effective action.

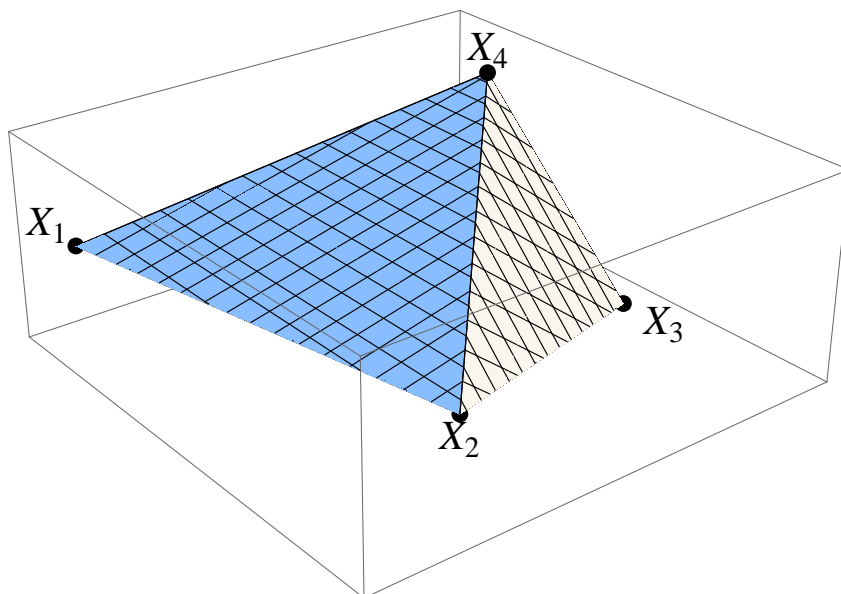


**Figure 1:** Fundamental domain of SU(4)

We start from the conjecture that the signal to noise ratio is maximized if  $\phi$  and  $\phi'$  are chosen, s.t. they are as far from the edges of the fundamental domain and each other as possible [1, 5, 6]. To find such points we first want to define a mapping which mirrors the point in the fundamental domain. We start by defining a mapping  $R_{i,j}(\phi)$  that reflects the points in the fundamental domain with respect to a  $(N - 2)$  dimensional hyperplane. The hyperplane  $R_{i,j}(\phi)$  goes through vertices  $\mathbf{X}_k, k \neq i, j$  and intersects the line connecting  $\mathbf{X}_i$  and  $\mathbf{X}_j$  at the middle. In figure 2 we show all the possible mappings  $R_{i,j}(\phi)$  on SU(4).

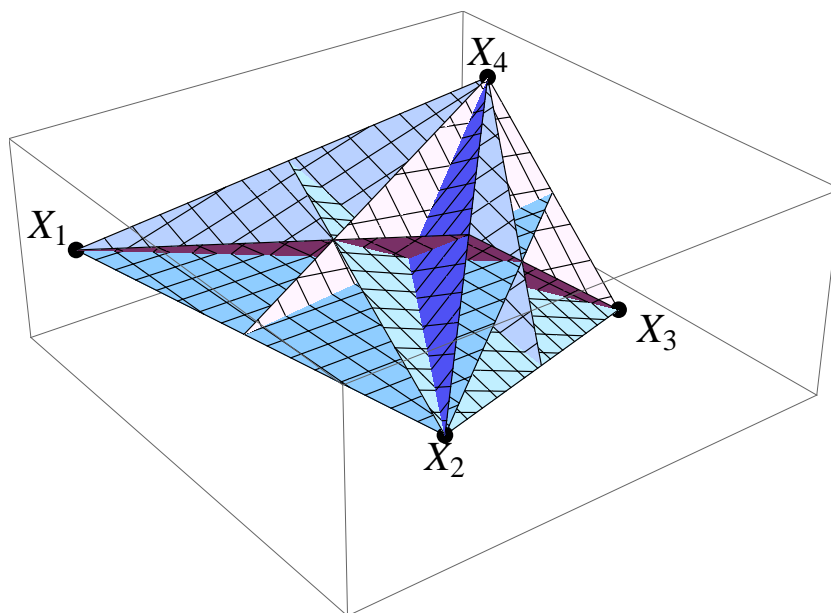


**Figure 2:** All possible  $R_{i,j}(\phi)$  hyperplanes on the fundamental domain of SU(4)

The function  $R_{i,j}(\phi)$  is not a mapping from the fundamental domain to itself, but we can define a composite mapping<sup>2</sup>

$$M(\phi) = (R_{1,N-1} \circ R_{2,N-2} \circ \dots \circ R_{[N/2],N-[N/2]})(\phi), \quad (3.3)$$

that has this property. The value of the field  $\phi'$  is then derived from  $\phi$  using  $M(\phi)$  which has a simple form  $\phi'_i = \phi_{N-i+1}$ .

We choose  $\phi$  to be in the middle of a line connecting  $\mathbf{X}_1$  and the centroid of the fundamental domain and associate a flow<sup>3</sup>

$$\begin{aligned} t(\eta) &= \frac{\eta N}{2\pi(N-2)} (\mathbf{X}_1 - \mathbf{X}_{N-1}) \\ &= \left( -\eta, \frac{2\eta}{N-2}, \dots, \frac{2\eta}{N-2}, -\eta \right), \end{aligned} \quad (3.4)$$

to the direction which gets mirrored by  $R_{1,N-1}(\phi)$  transformation and points outside from the fundamental domain. As an example boundary fields of SU(4) are

$$\phi = \begin{cases} -\eta - 9\pi/8, \\ \eta + \pi/8, \\ \eta + 3\pi/8, \\ -\eta + 5\pi/8, \end{cases} \quad \phi' = \begin{cases} \eta - 5\pi/8, \\ -\eta - 3\pi/8, \\ -\eta - \pi/8, \\ \eta + 9\pi/8. \end{cases} \quad (3.5)$$

Note that these boundary fields are different than those used in [1]. The possible improvement in the signal/noise ratio should be determined with lattice simulations.

#### 4. Boundary improvement

Improvement coefficient  $c_t$  is previously known for  $N = 2, 3$  to one loop order in perturbation theory. These values have been calculated by Lüscher et. al. in [5] for SU(2) and in [6] for SU(3) resulting in  $c_t^{(1,0)}(\text{SU}(2)) = -0.0543(5)$  and  $c_t^{(1,0)}(\text{SU}(3)) = -0.08900(5)$ . The method used in [5] and [6] is also applicable to  $N > 3$  with some modifications.

The details of the calculation of  $c_t^{(1,0)}$  will be given in [10]. The calculation goes along the lines of [5]. The idea of the process is to calculate  $p_{1,0}(L/a) = \frac{\partial \Gamma_1(L/a)}{\partial \eta} / \frac{\partial \Gamma_0(L/a)}{\partial \eta}$  from (2.6) as a function of the lattice size  $L/a$ . This is done by solving a second order difference relation to several different operators. In this way we are able to solve  $p_{1,0}(L/a)$  and consequently the running coupling  $g^2$  to one loop order in perturbation theory for a range in  $L/a \in \{6, 8, 10, \dots, 64\}$ .

The variable  $p_{1,0}(L/a)$  has an asymptotic expansion in  $L/a$  [5]

$$p_{1,0}(L/a) \sim \sum_{n=0}^{\infty} (r_n + s_n \ln(L/a)) \left(\frac{a}{L}\right)^n, \quad (4.1)$$

where  $s_0 = 2b_{0,0}$  and  $s_1 = 0$ . The coefficient  $c_t^{(1,0)}$  is determined by demanding linear cutoff effects to be absent in (4.1), i.e.  $r_1 = 2c_t^{(1,0)}$ . The problem is then to extract the coefficient  $r_1$  as accurately as possible from the  $p_{1,0}(L/a)$  data. To do this we used the "Blocking" method described in [7]. Our preliminary results are shown in table 1.

<sup>2</sup> $R_{i,i}(\phi)$  is the identity mapping and  $[x]$  means the integer part of  $x$

<sup>3</sup>The normalization  $\frac{\eta N}{2\pi(N-2)}$  is chosen such that the coefficients of  $\eta$  the standard case of SU(3).

$N$	$c_t^{(1,0)}$	$\delta c_t^{(1,0)}$
2	-0.0543	0.0002
3	-0.088	0.005
4	-0.1220	0.0002
5	-0.154	0.004
6	-0.1859	0.0008
7	-0.218	0.004
8	-0.249	0.004

**Table 1:** The values of  $c_t^{(1,0)}$  and estimated errors  $\delta c_t^{(1,0)}$  for  $N = 2, \dots, 8$ .

We expect  $c_t^{(1,0)} = AC_2(R) + BC_2(G) = \tilde{A}N + \tilde{B}/N$ . This is motivated by the fact that the Feynman diagrams involved are proportional to these Casimir invariants. Also it has been shown in [8] that the fermionic part of  $c_t^{(1)}$  is proportional to the Casimir invariant  $T(R)$ . See also [9]. A plot of the values of  $c_t^{(1,0)}$  as a function of  $N$  and our fit to the data is shown in 3.

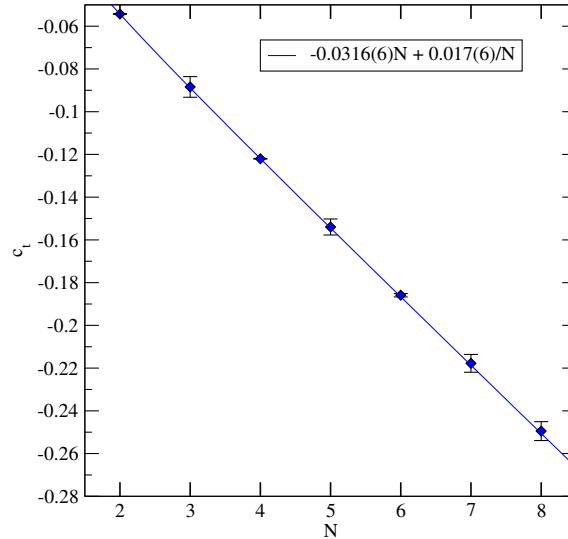


**Figure 3:**  $c_t^{(1,0)}$  as a function of  $\tilde{A}N + \tilde{B}/N$  fit to the data

We also want to be sure that setting  $c_t$  to the value that we obtained removes the  $\mathcal{O}(a)$  terms from the lattice step scaling function. This can be seen from figure 4 where we have plotted  $\delta_0$  as a function of  $(a/L)^2$ . After the improvement  $\delta_0$  behaves linearly which is a clear indication that the leading terms are of the order  $\mathcal{O}(a^2)$ .

## 5. Summary and outlook

We have investigated the boundary conditions in general  $N$  and calculated the  $\mathcal{O}(a)$  boundary improvement coefficients for  $N = 2, \dots, 8$  in the Schrödinger functional scheme. The precision in the determination of  $c_t^{(1,0)}$  can be increased by using more than double precision floating point numbers in the numerical calculations. We are currently implementing these enhancements to improve our results.

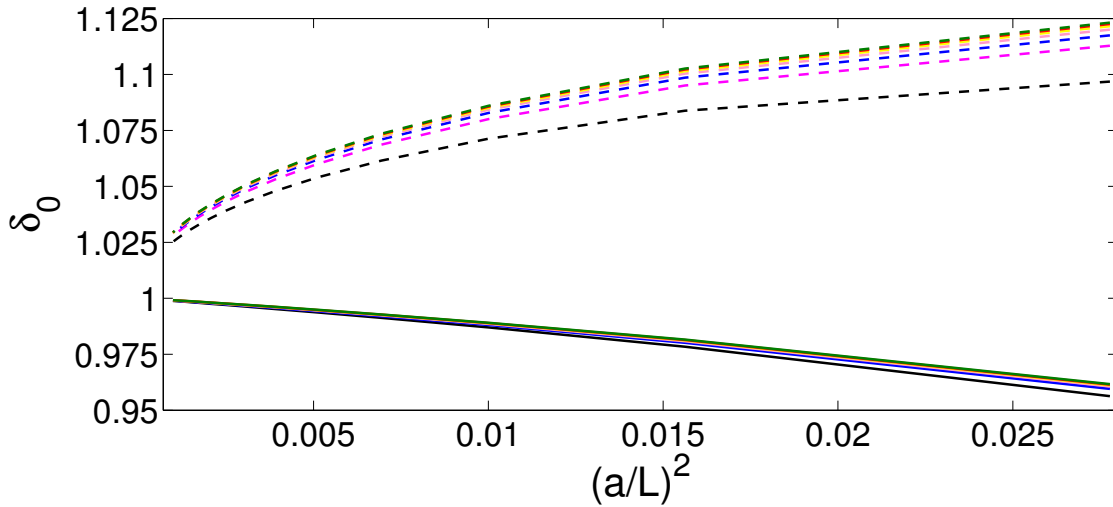


**Figure 4:** The unimproved (dashed) and improved (solid) one loop lattice step scaling function normalized to the continuum limit ( $\delta_0$ ) as a function of  $(a/L)^2$  for  $SU(N)$  pure gauge with  $N = 2$  (black), 3 (purple), 4 (blue), 5 (pink), 6 (yellow), 7 (red) and 8 (green).

## Acknowledgments

This work was supported by the Danish National Research Foundation DNRF:90 grant. TK is also funded by the Danish Institute for Advanced Study.

## References

- [1] B. Lucini and G. Moraitis, Phys. Lett. B **668**, 226 (2008) [arXiv:0805.2913 [hep-lat]].
- [2] T. DeGrand, Y. Shamir and B. Svetitsky, Phys. Rev. D **85**, 074506 (2012) [arXiv:1202.2675 [hep-lat]].
- [3] A. Hietanen and R. Narayanan, Phys. Rev. D **86**, 085002 (2012) [arXiv:1204.0331 [hep-lat]].
- [4] B. Lucini and M. Panero, Phys. Rept. 526 (2013) 93 [arXiv:1210.4997 [hep-th]].
- [5] M. Luscher, R. Narayanan, P. Weisz and U. Wolff, Nucl. Phys. B **384**, 168 (1992) [arXiv:hep-lat/9207009].
- [6] M. Luscher, R. Sommer, P. Weisz and U. Wolff, Nucl. Phys. B **413**, 481 (1994) [arXiv:hep-lat/9309005].
- [7] M. Luscher and P. Weisz, Nucl. Phys. B **266**, 309 (1986).
- [8] T. Karavirta, A. Mykkanen, J. Rantaharju, K. Rummukainen and K. Tuominen, JHEP **1106**, 061 (2011) [arXiv:1101.0154 [hep-lat]].
- [9] S. Sint and P. Vilaseca, PoS LATTICE **2012**, 031 (2012) [arXiv:1211.0411 [hep-lat]].
- [10] A. Hietanen, T. Karavirta and P. Vilaseca, In preparation